Electrosorption of Hexavalent Chromium Ions by MnO₂/Carbon Fiber Composite Electrode: Analysis and Optimization of the Process by Box-Behnken Design

Zainab M. Issa [a, *], Rasha H. Salman [a], and Prashant Basavaraj Bhagawati [b]

a Chemical Engineering Department, College of Engineering, University of Baghdad, Baghdad, Iraq
b College of Engineering and Technology, Ashta, Maharashtra, India

Abstract

A nano manganese dioxide (MnO₂) was electrodeposited galvanostatically onto a carbon fiber (CF) surface using the simple method of anodic electrodeposition. The composite electrode was characterized by field emission scanning electron microscopy (FESEM), and X-ray diffraction (XRD). Very few studies investigated the efficiency of this electrode for heavy metals removal, especially chromium. The electrosorption properties of the nano MnO₂/CF electrode were examined by removing Cr(VI) ions from aqueous solutions. NaCl concentration, pH, and cell voltage were studied and optimized using the Box-Behnken design (BDD) to investigate their effects and interactions on the electrosorption process. The results showed that the optimal conditions for the removal of Cr(VI) ions were a cell voltage of 4.6 V, pH of 2 and NaCl concentration of 1.5 g/L. This work indicated that MnO₂/CF electrode was highly effective in removing Cr(VI) ions and the BBD approach was a feasible and functional method for evaluating the experimental data.

1- Introduction

Development of industries to serve human needs increases as the population grows. This rise has a negative impact on the environment, human health, and aquatic life [1, 2]. Heavy metals are a source of pollution even at trace levels, with toxicity ranging from high to carcinogenicity due to repeated exposure [3, 4]. Metals are extremely dangerous since they are not biodegradable and may concentrate in biological organisms, getting denser as they go into the food chain. [5]. In industrial wastewater treatment, toxic heavy metals of particular concern are zinc, copper, nickel, mercury, cadmium, lead, and chromium [2, 6]. Chromium is a primary concern for the Environmental Protection Agency (EPA) especially when present in the hexavalent form, Because of its widespread application and high toxicity [7]. In industry, chromium compounds are utilized in electroplating, leather tanning, metal polishing, chemical manufacturing, pigments, electronic and electrical equipment [8]. Chromium typically enters the aquatic environment in two forms: Cr(III) and Cr(VI). In general, Cr(VI) is more dangerous than Cr (III). Furthermore, Cr(VI) is a strong oxidant that may be absorbed by the skin and is highly mobile in soeil and aquatic systems [9, 10]. The acceptable limits of Cr(VI) and total chromium (TCr) released to surface water should be less than 0.05 and 0.1 mg/l, respectively, according to the United States Environmental Protection Agency (USEPA) [2, 11]. Many strategies for removing Cr(VI) ions, including ion exchange, chemical precipitation, coagulation, chemical reduction, adsorption [4], and capacitive deionization (CDI) or electrosorption considered efficient methods [12]. Electrosorption is an electrochemical method of removing metals under the influence of an electric field. CDI is an electrosorption process in which ions in an aqueous solution are adsorbed on the electrical double layers of porous electrodes after being exposed to a low-voltage electric field [13, 14]. When compared to other existing desalination systems, CDI offers the benefits of being environmentally sustainable, utilizing less energy and having lower running costs than other desalination methods, and being simpler to regenerate and maintain [12]. The most important component of any electrochemical system is the electrode material [15]. Carbon aerogel, activated carbon, carbon fiber, ordered mesoporous carbon, carbon nanotubes, and graphene are examples of nanoporous carbon materials that have been suitable electrodes for the electrosorption process [16], [17]. Carbon fiber (CF) is a porous kind of activated carbon that has a strong electrosorptive capability owing to its larger specific surface area [14]. Carbon fiber has gotten attention because of its potentially inexpensive manufacturing cost, significant uptake capacity, high strength, high electrical conductivity, high stability, and consistent pore size [18, 19]. The capacitance of the

electrosorption process is a strong indicator of how effectively porous materials remove ions [20]. The electrochemical storing mechanism of metal ions in capacitive deionization operates in the same manner as an electrochemical supercapacitor. It is based on either the electrical double-layer capacitance (EDL) from pure electrostatic adsorption when porous carbon materials are used or the pseudo capacitance from reversible and fast faradic reactions when redox-active materials (pseudo capacitive materials) are used [21]. In surface-redox pseudo capacitive materials, ions are electrochemically adsorbed onto the surface of a material accompanied by a faradaic charge transfer [22]. An example of pseudo capacitive material is manganese dioxide, MnO_2 stores ions by the surface redox reaction between oxidation states of Mn^{4+} and Mn^{3+}. The mechanism is based on the adsorption of electrolyte cations (C^+) onto the surface of MnO_2 as shown in Eq. 1 [23]:

$$(MnO_2)_{surface} + C^+ + e^- \leftrightarrow (MnO_2^- \; C^+)_{surface} \qquad (1)$$
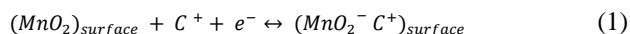
Where: C^+ represents an alkali metal cation (H^+, Li^+, Na^+, K^+) in the electrolyte.

Electrochemical pseudo capacitors could be constructed from a wide range of materials, including conducting polymers, noble metal oxides which including RuO_2 and IrO_2, and transition metal oxides like MnO_2, NiO, Co_2O_3, FeO, TiO_2, SnO_2, V_2O_5 and MoO [24]. Transition metal oxides offer pseudo-capacitance behavior, with a higher specific capacitance than electrical double layers of carbonaceous materials due to the faradaic redox reaction in the active materials. These active materials are loaded onto the surface of carbon to enhance the electrosorption capability of the carbon materials [25]. MnO_2 is a perspective electrode material for supercapacitors among metal oxide compounds because of its low cost, environmentally friendly nature, and relatively high theoretical pseudo capacitance value, 1370 F.g-1, which is much greater than that of carbon-based materials. So, a lot of interest has been focused on developing MnO_2-based materials as an electrode for electrochemical supercapacitors and as effective adsorbents to remove heavy metals from water. Numerous investigations have focused on connecting MnO_2 to the surface of carbonaceous materials, such as activated carbon, carbon fibers, carbon nanotubes, and graphene-based materials, to overcome this difficulty [26, 27].

Currently, relatively few articles have explored heavy metal removal by electrosorption onto MnO_2/CF electrodes, and no previous works have investigated the applicability of this electrode for chromium ion removal by electrosorption. The current study targets to synthesize and characterize MnO_2/carbon fiber electrode, the produced electrode's performance in electrosorption of Cr(VI) ions from an aqueous solution was examined by changing three variables cell voltage, pH, and ionic strength (NaCl concentration). The effect of these selected operational factors and their interactions on removal efficiency were studied and optimized using the response surface methodology and the Box-Behnken design.

2- Experimental Work

2.1. Reagents and Chemicals

All reagents were of analytical grade and were utilized without additional purification. For the electrodeposition of MnO_2, Manganese (II) sulfate monohydrate ($MnSO_4.H_2O$) (98% purity, THOMAS BAKER) and sulfuric acid (H_2SO_4) (98% purity, alpha chemika, India) were used in the electrolytic solution. For the experiment of chromium ions removal, potassium dichromate ($K_2Cr_2O_7$) (99% purity, alpha chemika, India), sodium chloride (NaCl) (99% purity, HiMedia Laboratories Pvt.Ltd.), sodium hydroxide (NaOH) (98% purity, alpha chemika, India), diphenylcarbazide ($C_{13}H_{14}N_4O$, Fluka Chemika, Switzerland), and HNO_3 (69% purity, Central Drug House (P) Ltd.) were utilized. All solutions were prepared with deionized water of 5μS/cm conductivity. The pure carbon fiber purchased form Jiaxing AGG composites Co. Ltd., China.

Fig. 1 shows the FESEM-EDX characterization of the purchased pure carbon fiber electrode. FESEM analysis depicts the smooth surface of pure carbon fiber electrode as shown in Fig. 1a and Fig. 1b. EDX analysis demonstrates that 86.76% of electrode material is composed of carbon as shown in the Fig. 1c.

2.2. Preparation of Electrodes

To synthesize nanostructured MnO_2, experiments of anodic electrodeposition of MnO_2 onto CF were carried out utilizing commercial CF as a substrate and current collector. A rectangular slice of CF (16.5cm × 5 cm) was activated for 30 minutes at 80°C with 5% HNO_3, then cleaned and stored in distilled water. The electrodeposition of MnO_2 onto CF was carried out galvanostatically for 4 h at a current density of (0.3 mA/cm^2) using a regulated DC power supply (UNI-T: UTP3315TF-L). A 2L beaker containing 1.8L of aqueous solution (0.64M H_2SO_4 + 0.35M $MnSO_4$) was used as the electrolytic solution. The solution was agitated and retained at 90 °C by a hot plate magnetic stirrer (Heidolph: MR Hei-standard, Germany). Three electrodes were used; an activated CF piece served as an anode, and two graphite served as counter electrodes. After the completion electrodeposition process, the composite electrode of MnO_2/CF was washed and rinsed multiple times with distilled water and then dried. The prepared electrode would be used later in the electrosorption process of chromium ions. The electrodeposition experimental setup is schematically shown in Fig. 2.

2.3. Characterization and Analysis

The crystal structure of deposited MnO_2 films were characterized by X-ray diffraction (XRD, Phillips: PW1730, USA), and the diffraction data were collected over 2θ. Cu-Kα radiation utilized as the X-ray source with λ = 1.54056 ˚A. The morphology and composition of the prepared MnO_2/CF electrode was tested using Field

emission scanning electron microscopy (FESEM, Tescan Mira3, Czech) equipped with an energy dispersive X-ray spectrometry (EDX) analyzer at an operating conditions of 25kV and 100μA.

The amount of Cr(VI) ions that remained in the aqueous solution was determined at the maximum wavelength of 540 nm using a UV spectrophotometer (Thermo UV-Spectrophotometer, USA). In acidic environments, diphenylcarbazide interacts with Cr(VI) ions to generate a dark violet-colored complex [28, 29].
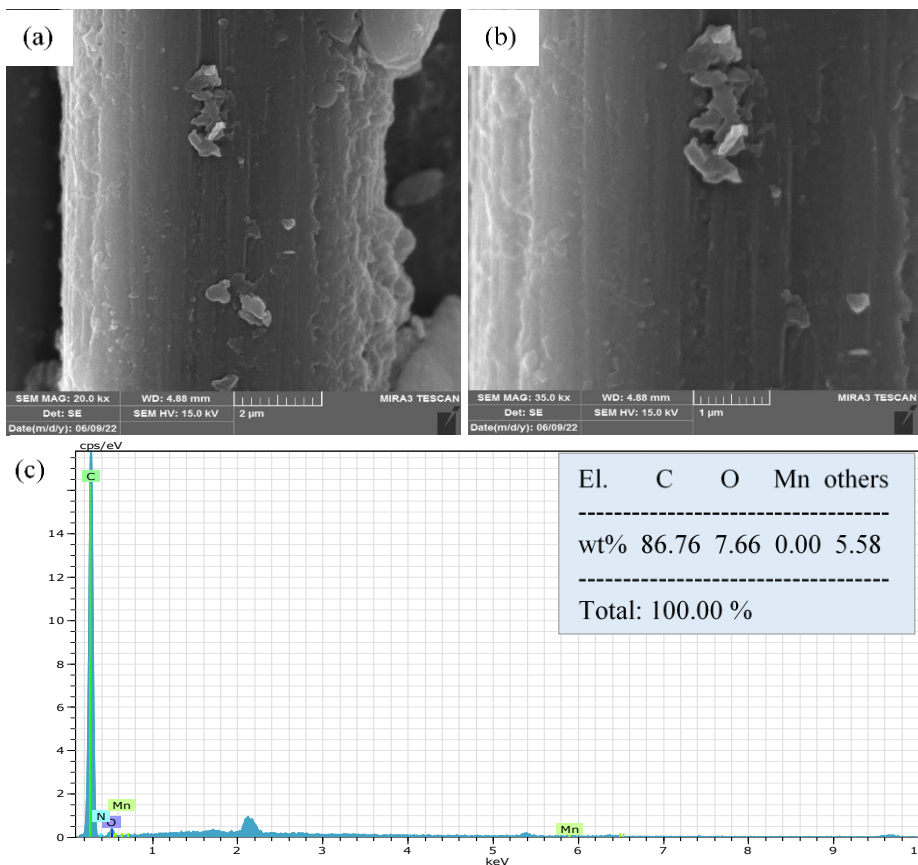
Fig. 1. Characterization of the Pure Carbon Fiber Electrode (a, b) FESEM (c) EDX
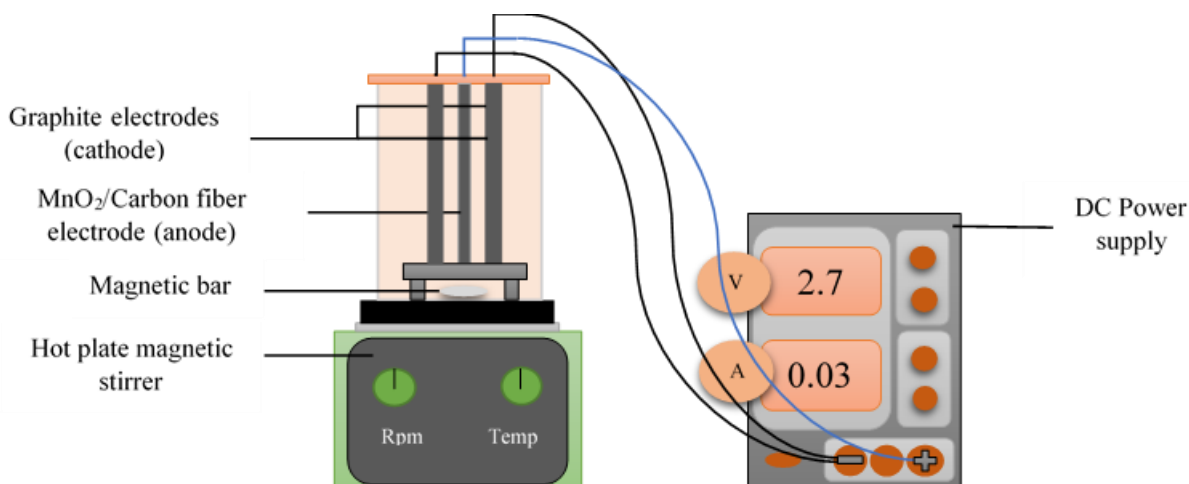
Fig. 2. Setup Scheme of the Electrodeposition Process

2.4. Electrosorption experiment

The electrosorption process was tested in a batch experiment consisting of a glass beaker comprising of an aqueous solution of 0.8L with a constant starting Cr(VI) ions concentration of 100 ppm to study the electrosorption characteristics of the nanostructured MnO_2/carbon fiber. The CDI system used two electrodes: a working electrode of MnO_2/CF and counter electrode of stainless steel plate (17cm x 5 cm x 3 mm), with a 1.5cm space between the

electrodes. The aqueous solution was agitated with a constant stirring rate of 250 rpm during the experiment using a hot plate magnetic stirrer (Heidolph: MR Hei-standard, Germany) to guarantee ionic diffusion, and all tests were carried out at 25°C ±1 room temperature. A direct-current power supply was coupled to the electrodes to supply the electrical current. Before each experiment, the pH was adjusted to the desired value by adding 1M of sodium hydroxide or 1M of sulfuric acid, and it was detected with a pH meter equipment (HANNA instrument, pHep: HI98107). Eqs. 2 and 3 were used to compute the removal efficiency of Cr(VI) ions and the

equilibrium adsorption capacity qe (mg/g), respectively [17]:

$$Re\% = \frac{(C_0 - C_e)}{C_o} \times 100 \tag{2}$$

$$q_e = \frac{C_0 - C_e}{m} \times v \tag{3}$$

Where C_0 (mg/l) and C_e (mg/l) are the initial and equilibrium chromium ion concentrations in the solution, respectively, m is the total mass of the electrode, and V is the volume of solution. The CDI experimental setup is schematically shown in Fig. 3.
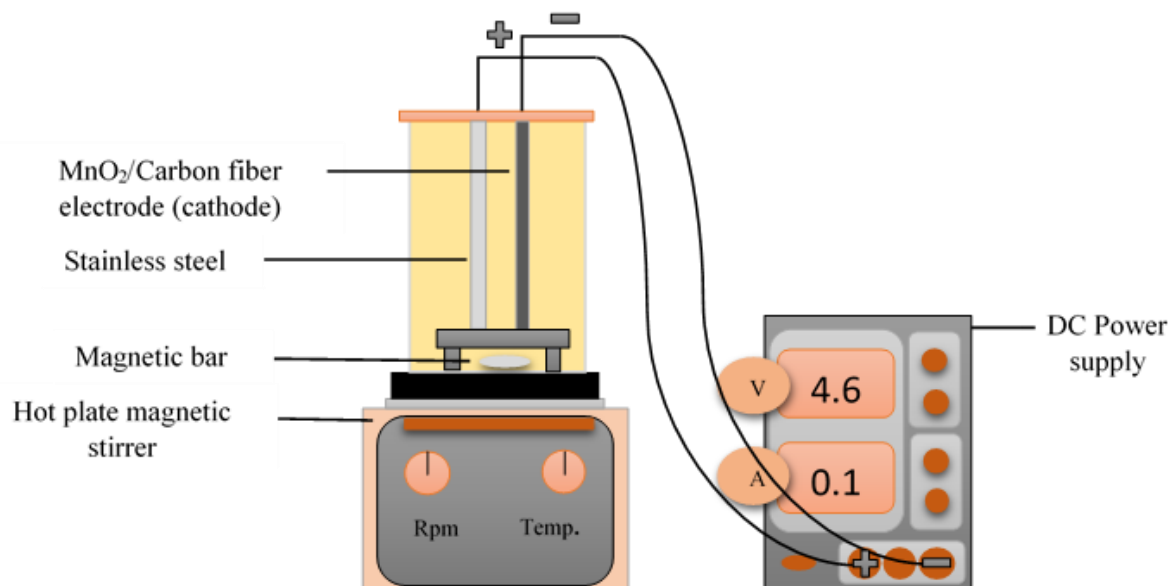
Fig. 3. Schematic Diagram of the Electrosorption Setup

2.5. Preliminary experiment

To determine the equilibrium time required for the MnO₂/carbon fiber electrodes to reach their saturation point, two preliminary batch electrosorption experiments were performed at pH 2, 4.1V, and 1g/L NaCl concentration with two initial concentrations (100 and 150 ppm of Cr ions). These two experiments were carried out before the set of experiments determined by the experimental design.

2.6. Experimental design

Response surface methodology (RSM) is a software program that consists of a set of a statistical and mathematical methods that are considered to be very effective for modeling and analyzing in which a response of interest is affected by numerous variables in order to investigate the optimal conditions to achieve the desired response [30].

A statistical design called Box-Behnken design (BBD) was used in this study to optimize and investigate the impact of specified operating variables on Cr(VI) ions removal using the electrosorption method. A Box-Behnken design of three-factors with three levels would

result in a set of 15 tests with three replicates at the center point [31]. The factors were pH (X1), NaCl concentration (X2), and cell voltage (X3), with the removal efficiency (Y) of Cr(VI) ions being the response. Generally, each variable in the Box-Behnken design has three levels as coded values, denoted by the numbers -1, 0 and 1. Levels 1 and -1 represent the maximum and minimum values for each input variable, respectively, while level 0 represents the variable's center value [17]. Table 1 displays the variables of the process with their coded and real values.

According to Eq. 4, the Box-Behnken design establishes a model of a polynomial second-order equation to analyze the influence of the specified variables on the produced response:

$$Y = \beta_o + \sum_{i=1}^{k} \beta_i X_i + \sum_{i=1}^{k} \beta_{ii} X_i^2 + \sum_{i=1}^{k} \sum_{j>1}^{k} \beta_{ij} X_i X_j \tag{4}$$

As previously stated, Y represents the achieved response (removal efficiency of Cr(VI) ions), βo is the intercept term, βi is the linear term, βii is the quadratic term, and βij is the interaction term, Xi, Xj, …, Xk are the process input variables [32].

Table 1. Coded and Real Values of Variables

Run	Blk	Coded values			Real values		
		X1	X2	X3	pH	NaCl	voltage
1	1	0	-1	1	4	0.5	4.6
2	1	1	0	1	6	1	4.6
3	1	0	0	0	4	1	4.1
4	1	0	0	0	4	1	4.1
5	1	0	1	-1	4	1.5	3.6
6	1	1	0	-1	6	1	3.6
7	1	0	-1	-1	4	0.5	3.6
8	1	-1	0	1	2	1	4.6
9	1	0	1	1	4	1.5	4.6
10	1	0	0	0	4	1	4.1
11	1	-1	1	0	2	1.5	4.1
12	1	-1	-1	0	2	0.5	4.1
13	1	-1	0	-1	2	1	3.6
14	1	1	-1	0	6	0.5	4.1
15	1	1	1	0	6	1.5	4.1

3- Result and Discussion

3.1. Characterization of MnO_2/carbon Fiber Composite Electrode

X-ray diffraction (XRD) analysis was used to determine the presence of deposited manganese dioxide nanoparticles on the carbon fiber surface, as well as their phases and crystal structure at 0.3 mA/cm^2, applied current density, and 0.64 M H_2SO_4 concentration. Fig. 4 shows the patterns of XRD analysis for MnO_2 nanostructured electrodeposited onto the carbon fiber surface.

The intensity of most diffraction peaks was for nanostructured MnO_2 with two diffraction peaks of pure carbon fiber, positioned approximately at 24º and 43º, which correspond to the amorphous carbon (002) and (100) lattice planes [23]. All of the electrodeposited MnO_2 diffraction peaks attributed to the pure phase of orthorhombic γ- MnO_2, and the peaks correspond with the standard JCPDS card (NO.14-0644) [33]. The diffraction peaks were at 2θ (34.2º, 37.16º, 38.24º, 42.44º, 44.04º, 56.32º, 57.8º, 61.69º, 65.24º, 69.08º, 71.96º, 75.72º, and 78.88º) as shown in Fig. 4.

Numerous studies have shown that electrode efficiency, capacity, and stability are greatly influenced by electrode morphology [34]. MnO_2 nanostructures electrodeposited on the surface of carbon fiber have the morphology of spherical brushes consisting of straight nanorods grown normally to the surface of carbon fiber, this has also observed by Xie et al. [35] and illustrated in Fig. 5. These several nanorods have approximately a smaller diameter (35.11 nm), they are merged to form a smooth and thin film. This film has a uniform structure and high capacity as a result of its large surface area. Furthermore, rod-like shapes can supply both ions and electrons with short diffusion channel lengths as well as adequate porosity for electrolyte penetration, resulting in rapid charge/discharge rates [36].
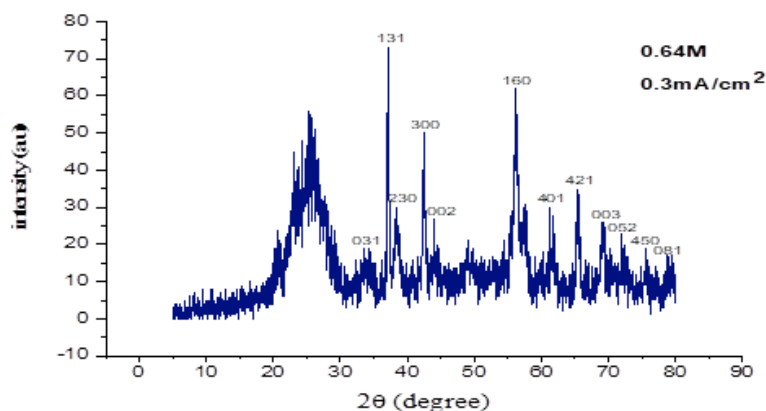
Fig. 4. Results of XRD Analysis of MnO_2 Nanoparticles Deposited on Carbon Fiber Prepared at (0.3mA/cm^2, 0.64M H_2SO_4)
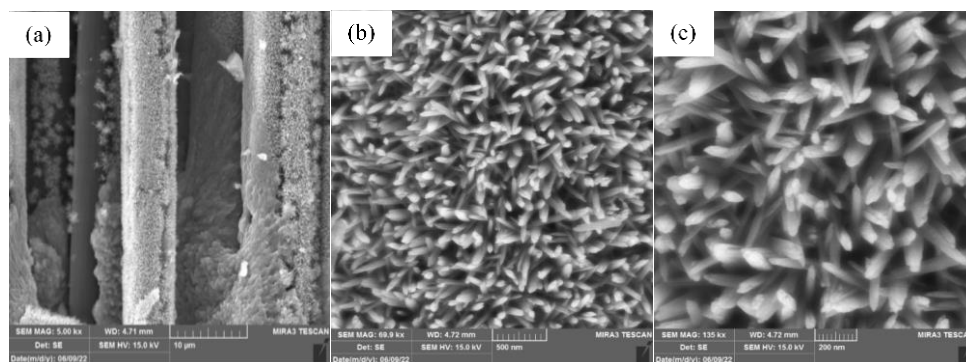
Fig. 5. Results of FESEM Image of MnO_2 Nanoparticles Deposited on Carbon Fiber Prepared at (0.3mA/cm^2, 0.64M H_2SO_4) with Different Magnifications (a) 10 μm, (b) 500nm and (c) 200 nm

3.2. Result of preliminary experiment

At pH = 2, cell voltage = 4.1V, and NaCl concentration = 1g/L, two preliminary experiment were accomplished. Adsorption for MnO$_2$/carbon fiber electrode was allowed to proceed for up to 5 h with periodic measurements, and it was revealed that adsorption for 4 h was sufficient to achieve equilibrium with high removal efficiency as shown in Fig. 6.

Since the equilibrium time for the two concentrations (100 and 150 ppm) were the same, 100 ppm concentration has been used as the initial concentration in all experiments that have been studied in the experimental design.

MnO$_2$/carbon fiber electrode could accelerate the electrosorption process to complete in 3 h according to its faradic-capacitive behavior. While due to the capacitive behavior of carbon fiber electrode, the electrosorption process require 4 h to reach the equilibrium time, that result has been achieved in our previous study [37].
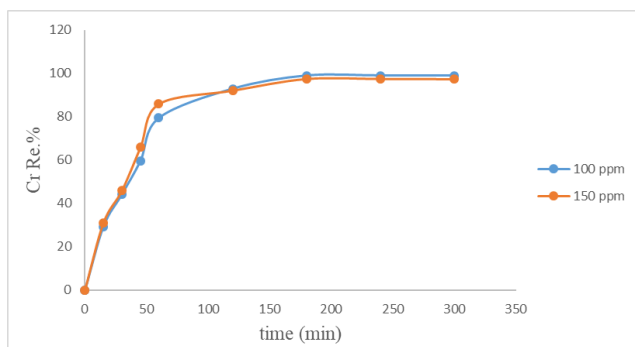
Fig. 6. The Removal Efficiency of Cr(VI) Ions vs. Time on MnO$_2$/Carbon Fiber Electrode at Conditions of pH 2, 4.1V, and 1 g/L NaCl Concentration

3.3. Analysis for electrosorption process using Response surface methodology

3.3.1. The Box–Behnken model

Table 2 displays the actual values achieved from the experimental work as well as the predicted values measured using RSM methods, which illustrate the electroporation process's response to the chromium ion removal efficiency [38]. Minitab-19 software was used to analyze experimental data. To establish the regression equation, the experimental data were fitted into a second-order model. Equation 5 gives the final empirical equation that shows the relation between the removal efficiency of Cr(VI) ions and the three specified variables in terms of coded units:

$$Y\% = 245.0 - 39.42X1 - 115.2X2 - 38.0X3 + 3.223X1^2 + 5.66X2^2 + 2.56X3^2 + 1.492X1*X2 + 1.829X1*X3 + 28.59X2*X3 \quad (5)$$

Where Y represents the removal % of Cr(VI) ions, i.e. the response, and the operational variables are pH (X1), NaCl concentration (X2), and cell voltage (X3).

The analysis of variance (ANOVA) based on the BBD was studied to evaluate the significance and suitability of the recommended polynomial quadratic models [39]. The degree of freedom (DOF), percentage contribution%, sum of squares (SS), mean of squares (MS), adjusted sum of squares (Adj. SS), adjusted mean of squares (Adj. MS), F-value, and P-value were used to specify the ANOVA analysis.

Table 3 displays the ANOVA results. ANOVA provides the percentage contribution for each variable, as shown in Table 3. The greater a variable's percentage contribution, the greater its impact to the final results. Any small change in its value will have a significant impact on the reaction [30]. ANOVA analysis shows that the contributions of pH, NaCl concentration and cell voltage are the same approximately, which mean that their impact on the response were convergent. The contribution of linear term was 71.48%, while the terms of square and two-way interaction have contributed with 20.42% and 7.52%, respectively. The model is highly significant, as demonstrated by lower P-values (p model = 0.000) and higher F-values (F model = 96.06). The ratio of mean square model (MS) to the error mean square represent the F-value. The higher the ratio, the higher the F-value [40]. In the model, the Probability value (P-value) is used to evaluate statistically significant effects. A P-value of less than 0.05 refers that the impact of the variable is statistically significant at a 95% confidence level [41]. Analysis of F-value and P-value indicated that pH (X1), NaCl (X2), voltage (X3) and pH*pH (X1*X1) terms are the most controlling terms in the model. Furthermore, high determination coefficient (R^2) which equal to 99.42% indicating good model fitting with experimental data.

3.3.2. Main effect plots

The relationship between the response and the selected operational variable could be illustrated using the main effect plots. Fig. 7 demonstrates the impacts of pH solution, cell voltage, and ionic strength on the removal efficiency of Cr(VI) ion in the electrosorption process using MnO$_2$/carbon fiber electrode, respectively.

The maximum removal efficiency was observed when the pH value was reduced to 2. The influence of pH was investigated from 2 to 6. Fig. 7 also demonstrates an obvious improvement in removal % when NaCl concentration increases from 0.5 to 1.5 g/L and applied voltage increases from 3.6 to 4.6V. The experimental results reveal that reducing the pH value improves the reduction of Cr(VI), whereas increasing the pH decreases the reduction of Cr(VI) due to the smaller amount of H$^+$ ion in the solution [42]. Because the presence of H$^+$ ions induces the cathodic reduction of Cr(VI) to Cr(III) under highly acidic environment, as indicated in Eqs. 6 and 7 [43]:

$$Cr_2O_7{}^{2-} + 8H^+ + 6e^- \rightarrow Cr_2O_3 + 4H_2O \qquad E°= 1.33 \text{ V} \qquad (6)$$

$$HCrO_4{}^- + 7H^+ + 3e^- \rightarrow Cr^{3+} + 4H_2O \qquad E°=1.35 \text{ V} \qquad (7)$$

Table 2. Experimental Results of BBD for Cr(VI) Ions Removal

Run	Blk	conc.	VoltagepH	NaCl	Re%		AC(mg/g)
		X1	X2	X3	Act.%	Pred.%	
1	1	4	0.5	4.6	64.510	64.493	83.23871
2	1	6	1	4.6	83.717	85.324	108.0219
3	1	4	1	4.1	69.901	69.804	90.19484
4	1	4	1	4.1	69.807	69.804	90.07355
5	1	4	1.5	3.6	64.914	64.931	83.76
6	1	6	1	3.6	63.027	62.768	81.32516
7	1	4	0.5	3.6	58.040	59.888	74.89032
8	1	2	1	4.6	99.990	100.249	129.0194
9	1	4	1.5	4.6	99.970	98.122	128.9935
10	1	4	1	4.1	69.703	69.804	89.93935
11	1	2	1.5	4.1	99.990	101.580	129.0194
12	1	2	0.5	4.1	85.469	85.227	110.2826
13	1	2	1	3.6	86.615	85.008	111.7613
14	1	6	0.5	4.1	65.251	63.661	84.19484
15	1	6	1.5	4.1	85.739	85.981	110.631

Table 3. Analysis of Variance for Cr(VI) Removal Using MnO_2/Carbon Fiber Electrode

Source	DOF	Seq. SS	Contribution	Adj. SS	Adj.MS	F-Value	P-Value
Model	9	2994.22	99.42%	2994.22	332.691	96.05	0.000
Linear	3	2152.61	71.48%	2152.61	717.537	207.15	0.000
pH	1	690.62	22.93%	690.62	690.619	199.38	0.000
NaCl	1	747.74	24.83%	747.74	747.742	215.87	0.000
voltage	1	714.25	23.72%	714.25	714.250	206.20	0.000
Square	3	615.04	20.42%	615.04	205.015	59.19	0.000
pH*pH	1	606.60	20.14%	613.83	613.834	177.21	0.000
NaCl*NaCl	1	6.93	0.23%	7.39	7.392	2.13	0.204
voltage*voltage	1	1.51	0.05%	1.51	1.512	0.44	0.538
2-Way Interaction	3	226.57	7.52%	226.57	75.523	21.80	0.003
pH*NaCl	1	8.90	0.30%	8.90	8.901	2.57	0.170
pH*voltage	1	13.38	0.44%	13.38	13.377	3.86	0.107
NaCl*voltage	1	204.29	6.78%	204.29	204.290	58.98	0.001
Error	5	17.32	0.58%	17.32	3.464		
Lack-of-Fit	3	17.30	0.57%	17.30	5.766	587.86	0.002
Pure Error	2	0.02	0.00%	0.02	0.010		
Total	14	3011.54	100.00%				

Model summery	S	R^2	R^2 (adj.)	PRESS	R^2 (pred.)	AICc	BIC
	1.86113	99.42%	98.39%	276.836	90.81%	154.72	74.51
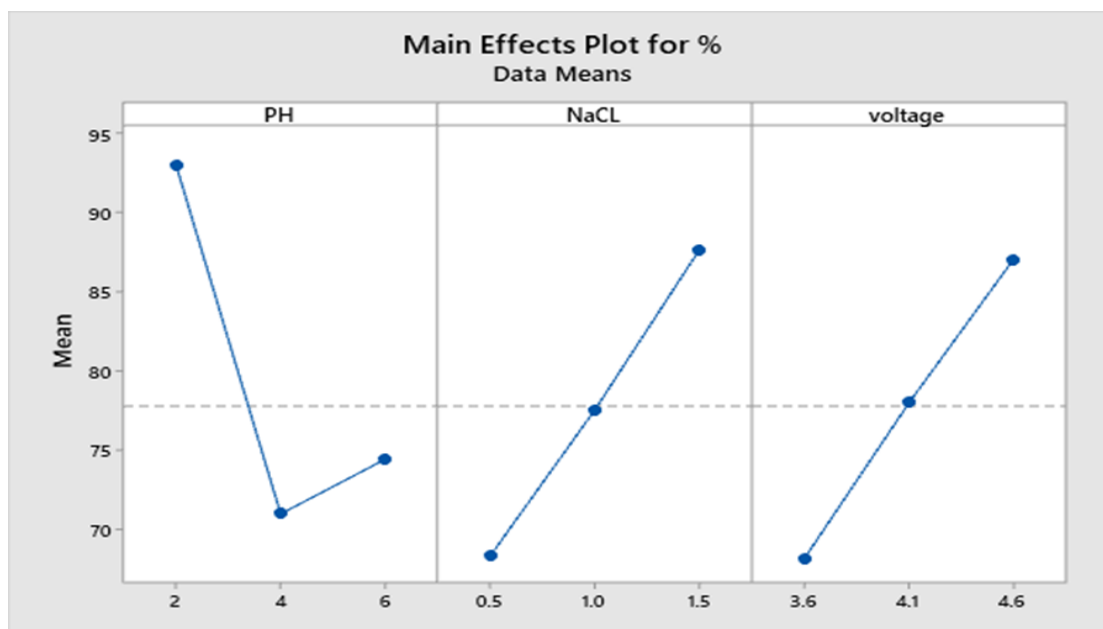
Fig. 7. Main Effect Plot for Cr(VI) Ions Removal Using MnO_2/Carbon Fiber Electrode

Furthermore, at higher pH levels, the following reaction occurs (Equation 8), and chromium could also generate hydroxide in the form of $Cr(OH)_3$.

$$Cr^{3+} + 3OH \rightarrow Cr(OH)_3 \tag{8}$$
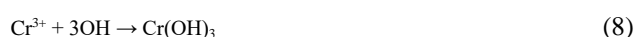
This reaction occurs quickly at higher pH levels and prevents Cr(VI) reduction [43].

The positive influence of increasing NaCl concentration on removal efficiency could be attributed to an increases in system electric current, ion flow, and redox reaction. However, further increases in NaCl concentration may result in inhabitation behavior, lowering or even suppressing chromium adsorption due to competing forces [44]. These effects have been examined because both natural water and wastewater typically include ions that can affect and compete with the adsorption of other ions [45].

The effects of increasing the applied voltage in this Figure reveals that increasing the applied voltage has a significant effect on the efficiency of Cr(VI) ions removal. An increase in electron flow velocity at high applied voltage values leads to an increase in electrostatic attraction and as a result the removal efficiency increase [46].

3.3.3. Effect of interactive parameters

Fig. 8a depicts the interaction between pH value and NaCl concentration and their impact on removal efficiency. As seen in the surface plot, increasing the pH value causes an obvious decrease in removal efficiency at 0.5 g/L NaCl concentration, whereas the decrease in removal efficiency is less at 1.5 g/L NaCl concentration. Furthermore, at pH 2, greater removal efficiency is obtained by increasing NaCl concentration to 1.5 g/L, however at pH 4, there is a significant reduction followed by a slight elevation at pH 6. The related contour plot shows a dark red region that represents the greatest removal effectiveness at pH 2 and NaCl concentration ranges of 0.8 to 1.5 g/L.

The interaction between pH value and cell voltage and their impact on removal efficiency is depicted in Fig. 8b, which shows that at pH= 2, higher removal efficiency was achieved when the cell voltage was 4.6V, followed by a gradual decrease in removal efficiency when the applied voltage was reduced to 3.6V. At a cell voltage of 3.6V, the Fig. reveals a severe reduction in removal efficiency as the pH value increases, and this decrease appears to be reduced as the cell voltage rises from 3.6 to 4.6V. According to the related contour plot, the area of highest removal efficiency values appears to be confined to cell voltages of (3.9-4.5V) and pH values of 2.

The effects of cell voltage and NaCl content on removal efficiency are depicted in Fig. 8c. At 1.5 g/L NaCl concentration, the removal efficiency of Cr(VI) ions increases linearly and reaches its maximum when the cell voltage is increased from 3.6 to 4.6V, however there is no significant influence of cell voltage at 0.5 g/L NaCl concentration. At a cell voltage of 3.6V, increasing NaCl concentration has no influence on removal efficiency, however at a cell voltage of 4.6V, increasing NaCl concentration from 0.5 to1.5 g/L increases removal efficiency. The resulting contour plot shows that the greatest removal efficiency values are found in the cell voltage range of 4.3-4.6V and the NaCl concentration range of 1.28-1.5g/L.

3.3.4. Optimization using desirability function and conformation test

To analyze the results and attain the optimal conditions for reducing Cr(VI) ions from an aqueous solution, optimization utilizing overall desirability was devised. The desirability function offers information on the quality and acceptability of the process [47]. The function represent a mathematical strategy for simultaneously determining the optimum values of input variables and output (response) by applying the optimum input variable levels [48]. When the desirability function ranges from 0 to 1, the removal efficiency is maximized. If the desirability value is 0, the proposed value is unfavorable. If it is 1, it signifies that the system's response has improved and it is stable [49].

To achieve this purpose, the three examined variables were estimated on a specified range of values, with the response aiming for the maximum. The optimization results for MnO₂/carbon fiber electrode are provided in Table 4, with the model having a desirability function of (1).

Two conformation experiments were performed using the program's recommended optimal parameters. The results of these experiments are intended to fit within the parameters determined by the optimization analysis. Table 5 shows the confirmation test results on optimally specified variables. The average removal efficiency was 99.98%, which was extremely near to the suggested one.

Table 4. Optimization of System Variables for the Maximum Removal of Cr(VI) Using MnO₂/Carbon Fiber Electrode

Response	Goal	Lower	Target		Upper	Weight	Importance
Cr removal%	Maximum	58.04	99.99			1	1
Solution of parameters			**Multiple response Prediction**				
pH	NaCl	voltage	Cr removal% (Fit)	Composite Desirability	SE Fit	95% CI	95% PI
2	1.5	4.6	116.986	1	2.20	(111.33, 122.64)	(109.58, 124.39)

Table 5. Confirmation Tests of Cr(VI) Ions Removal Using MnO₂/ Carbon Fiber Electrode

Run	pH	NaCl concentration	Cell voltage	Re% Actual	Average	AC (mg/g)
1	2	1.5	4.6	99.99%	99.98%	129.0194
2	2	1.5	4.6	99.98%		128.9806
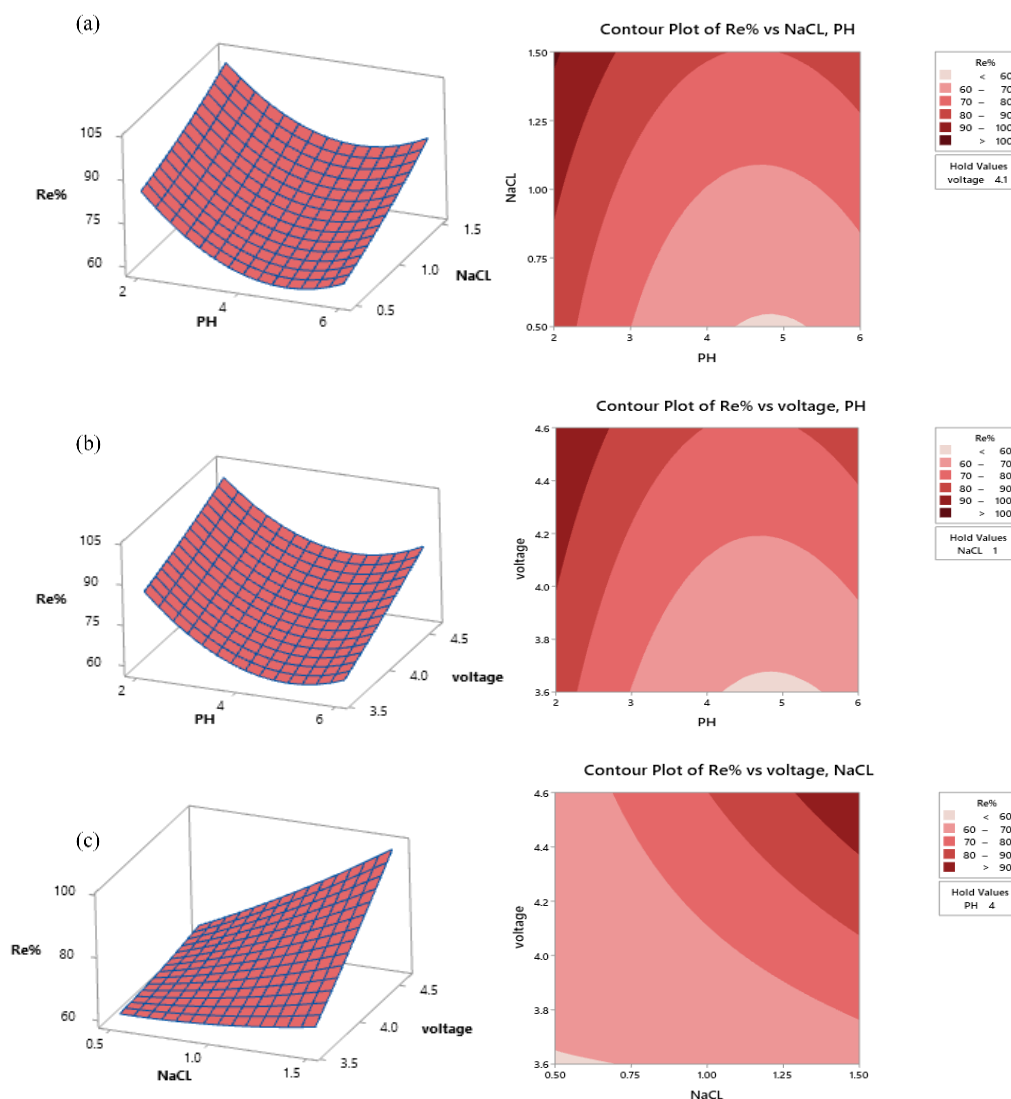
Fig. 8. Response Surface Plot and Contour Plot for the Effect of (a) pH and NaCl Concentration (g/L), (b) pH and Cell Voltage (V), and (c) NaCl Concentration (g/L) and Cell Voltage (V) on Cr(VI) Removal Using MnO_2/ Carbon Fiber Electrode

4- Conclusion

A Manganese dioxide/CF composite electrode has been efficiently synthesized by anodic electrodeposition process at 0.64 M H_2SO_4 concentration, 0.35 M $MnSO_4$ concentration and 0.3 mA/cm^2 current density. XRD and FESEM analysis confirm the formation of γ- MnO_2 nanorods with diffraction peaks of sharp intensity and smaller diameter of about 35.11nm. The electrosorption ability of MnO_2/carbon fiber electrode to adsorb Cr(VI) ions from an aqueous solution were investigated and the result showed a high removal efficiency of 99.99% and adsorption capacity of 129.0194 mg/g at concentration of 100 mg/l. From response surface methodology analysis, it has been detected that NaCl concentration has the major effect on removal efficiency with a contribution percentage of 24.83%. The optimization analysis of selected variables reveals that the optimal working conditions for electrosorption of Cr(VI) ions on MnO_2/carbon fiber electrode were at pH=2, cell voltage= 4.6V, and NaCl concentration= 1.5 g/L, which was determined using the BDD.

Nomenclature

Symbols	Description	Units
AC	Adsorption capacity	mg/g
C_e	Equilibrium concentration	mg/l
C_o	Initial concentration	mg/l
m	Total mass of the electrode	g
q_e	Adsorption capacity	mg/g
R^2	Determination coefficient	-
Re	Removal efficiency	%
$X1$	Real pH value	-
$X2$	Real NaCl Concentration value	g/L
$X3$	Real applied voltage value	V
X_i	input variables of the process	-
X_j	input variables of the process	-
X_k	input variables of the process	-

Y	Response (removal efficiency)	%

Greek Letters	Description	Units
β	Phase of MnO_2	-
β_o	intercept term	-
β_i	linear term	-
β_{ii}	quadratic term	-
β_{ij}	interaction term	-
γ	Phase of MnO_2	-
θ	Angle	radian
λ	wavelength	A°
v	Volume of aqueous solution	m^3

Abbreviation

Symbol	Description
Adj.MS	Adjusted mean of square
Adj.SS	Adjusted sum of square
AFM	Atomic force microscopy
ANOVA	Analysis of variance
BBD	Box–Behnken design
CDI	Capacitive deionization
CF	Carbon fiber
DC	Direct current
DOF	Degree of freedom
EDL	Electrical double layer
EDX	Energy-dispersive X-ray spectrometry
FESEM	Field emission scanning electronic microscopy
MS	Mean of square
RSM	Response surface methodology
SS	Sum of Square
UV	Ultraviolet–visible
XRD	X-ray diffraction

References

[1] M. S. Gaikwad and C. Balomajumder, "Current Progress of Capacitive Deionization for Removal of Pollutant Ions," *Electrochem. Energy Technol.*, vol. 2, no. 1, pp. 17–23, 2016, https://doi.org/10.1515/eetech-2016-0004.

[2] L. Chen, C. Wang, S. Liu, and L. Zhu, "Investigation of adsorption/desorption behavior of Cr(VI) at the presence of inorganic and organic substance in membrane capacitive deionization (MCDI)," *J. Environ. Sci.*, pp. 1–12, 2019, https://doi.org/10.1016/j.jes.2018.11.005.

[3] R. Chen, T. Sheehan, J. L. Ng, M. Brucks, and X. Su, "Capacitive deionization and electrosorption for heavy metal removal," *Environ. Sci. Water Res. Technol.*, vol. 6, no. 2, pp. 258–282, 2020, https://doi.org/10.1039/C9EW00945K.

[4] H. Peng, Y. Leng, and J. Guo, "Electrochemical removal of chromium (VI) from wastewater," *Appl. Sci.*, vol. 9, no. 6, 2019, https://doi.org/10.3390/app9061156.

[5] C. E. Barrera-Díaz, V. Lugo-Lugo, and B. Bilyeu, "A review of chemical, electrochemical and biological methods for aqueous Cr(VI) reduction," *J. Hazard. Mater.*, vol. 223–224, pp. 1–12, 2012, https://doi.org/10.1016/j.jhazmat.2012.04.054.

[6] H. Barabadi, S. Honary, P. Ebrahimi, A. Alizadeh, F. Naghibi, and M. Saravanan, "Optimization of myco-synthesized silver nanoparticles by response surface methodology employing Box-Behnken design," *Inorg. Nano-Metal Chem.*, vol. 49, no. 2, pp. 33–43, 2019, https://doi.org/10.1080/24701556.2019.1583251.

[7] X. Su, A. Kushima, C. Halliday, J. Zhou, J. Li, and T. A. Hatton, "Electrochemically-mediated selective capture of heavy metal chromium and arsenic oxyanions from water," *Nat. Commun.*, vol. 9, no. 1, 2018, https://doi.org/10.1038/s41467-018-07159-0.

[8] D. E. Kimbrough, Y. Cohen, A. M. Winer, L. Creelman, and C. Mabuni, "A critical assessment of chromium in the environment," *Crit. Rev. Environ. Sci. Technol.*, vol. 29, no. 1, pp. 1–46, 1999, https://doi.org/10.1080/10643389991259164.

[9] P. K. Ghosh, "Hexavalent chromium [Cr(VI)] removal by acid modified waste activated carbons," *J. Hazard. Mater.*, vol. 171, no. 1–3, pp. 116–122, 2009, https://doi.org/10.1016/j.jhazmat.2009.05.121.

[10] L. Khezami and R. Capart, "Removal of chromium (VI) from aqueous solution by activated carbons: Kinetic and equilibrium studies," *J. Hazard. Mater.*, vol. 123, no. 1–3, pp. 223–231, 2005, https://doi.org/10.1016/j.jhazmat.2005.04.012.

[11] A. Baral and R. D. Engelken, "Chromium-based regulations and greening in metal finishing industries in the USA," *Environ. Sci. Policy*, vol. 5, no. 2, pp. 121–133, 2002, https://doi.org/10.1016/S1462-9011(02)00028-X.

[12] M. S. Gaikwad and C. Balomajumder, "Simultaneous electrosorptive removal of chromium(VI) and fluoride ions by capacitive deionization (CDI): Multicomponent isotherm modeling and kinetic study," *Sep. Purif. Technol.*, 2017, https://doi.org/10.1016/j.seppur.2017.06.017.

[13] A. Thamilselvan, A. S. Nesaraj, and M. Noel, "Review on carbon-based electrode materials for application in capacitive deionization process," *Int. J. Environ. Sci. Technol.*, vol. 13, no. 12, pp. 2961–2976, 2016, https://doi.org/10.1007/s13762-016-1061-9.

[14] R. Rajumon, S. P. Aravind, S. Bhuvaneshwari, J. Ranjitha, and P. Mohanraj, "Removal of cadmium heavy metal ions from wastewater by electrosorption using modified activated carbon felt electrodes," *Water Sci. Technol.*, vol. 82, no. 7, pp. 1430–1444, 2020, https://doi.org/10.2166/wst.2020.425.

[15] Y. Zhang *et al.*, "Progress of electrochemical capacitor electrode materials: A review," *Int. J. Hydrogen Energy*, vol. 34, no. 11, pp. 4889–4899, 2009, https://doi.org/10.1016/j.ijhydene.2009.04.005.

[16] C. H. Hou and C. Y. Huang, "A comparative study of electrosorption selectivity of ions by activated carbon electrodes in capacitive deionization," *Desalination*, vol. 314, pp. 124–129, 2013, https://doi.org/10.1016/j.desal.2012.12.029.

[17] J. T. Hasan and R. H. Salman, "Electrosorption of cadmium ions from the aqueous solution by a MnO2/carbon fiber composite electrode," *Desalin. Water Treat.*, vol. 243, pp. 187–199, 2021, http://doi.org/10.5004/dwt.2021.27885.

[18] L. Huang, S. Zhou, F. Jin, J. Huang, and N. Bao, "Characterization and mechanism analysis of activated carbon fiber felt-stabilized nanoscale zero-valent iron for the removal of Cr(VI) from aqueous solution," *Colloids Surfaces A Physicochem. Eng. Asp.*, vol. 447, pp. 59–66, 2014, https://doi.org/10.1016/j.colsurfa.2014.01.037.

[19] X. Zhao, B. Jia, Q. Sun, G. Jiao, L. Liu, and D. She, "Removal of Cr6þ ions from water by electrosorption on modified activated carbon fibre felt," *R. Soc. Open Sci.*, vol. 5, no. 9, 2018, https://doi.org/10.1098/rsos.180472.

[20] C. H. Hou, C. Liang, S. Yiacoumi, S. Dai, and C. Tsouris, "Electrosorption capacitance of nanostructured carbon-based materials," *J. Colloid Interface Sci.*, vol. 302, no. 1, pp. 54–61, 2006, https://doi.org/10.1016/j.jcis.2006.06.009.

[21] Y. H. Liu, H. C. Hsi, K. C. Li, and C. H. Hou, "Electrodeposited manganese dioxide/activated carbon composite as a high-performance electrode material for capacitive deionization," *ACS Sustain. Chem. Eng.*, vol. 4, no. 9, pp. 4762–4770, 2016, https://doi.org/10.1021/acssuschemeng.6b00974.

[22] V. Augustyn, P. Simon, B. Dunn, V. Augustyn, P. Simon, and B. Dunn, "Pseudocapacitive oxide materials for high-rate electrochemical energy storage," *Energy Environ. Sci.*, vol. 7, pp. 1597–1614, 2014, https://doi.org/10.1039/C3EE44164D.

[23] M. Liu, L. Gan, W. Xiong, Z. Xu, D. Zhu, and L. Chen, "Development of MnO2/porous carbon microspheres with a partially graphitic structure for high performance supercapacitor electrodes," *J. Mater. Chem. A*, vol. 2, no. 8, pp. 2555–2562, 2014, http://doi.org/10.1039/c3ta14445c.

[24] B. Babakhani and D. G. Ivey, "Anodic deposition of manganese oxide electrodes with rod-like structures for application as electrochemical capacitors," *J. Power Sources*, vol. 195, no. 7, pp. 2110–2117, 2010, https://doi.org/10.1016/j.jpowsour.2009.10.045.

[25] Z. Ye, T. Li, G. Ma, X. Peng, and J. Zhao, "Morphology controlled MnO2 electrodeposited on carbon fiber paper for high-performance supercapacitors," *J. Power Sources*, vol. 351, pp. 51–57, 2017, https://doi.org/10.1016/j.jpowsour.2017.03.104.

[26] Y. H. Liu, T. C. Yu, Y. W. Chen, and C. H. Hou, "Incorporating Manganese Dioxide in Carbon Nanotube-Chitosan as a Pseudocapacitive Composite Electrode for High-Performance Desalination," *ACS Sustain. Chem. Eng.*, vol. 6, no. 3, pp. 3196–3205, 2018, https://doi.org/10.1021/acssuschemeng.7b03313.

[27] C. Hu, F. Liu, H. Lan, H. Liu, and J. Qu, "Preparation of a manganese dioxide/carbon fiber electrode for electrosorptive removal of copper ions from water," *J. Colloid Interface Sci.*, vol. 446, pp. 380–386, 2015, https://doi.org/10.1016/j.jcis.2014.12.051.

[28] K. Selvi, S. Pattabhi, and K. Kadirvelu, "Removal of Cr(VI) from aqueous solution by adsorption onto activated carbon," *Bioresour. Technol.*, vol. 80, no. 1, pp. 87–89, 2001, https://doi.org/10.1016/S0960-8524(01)00068-2.

[29] P. Lakshmipathiraj, G. Bhaskar Raju, M. Raviatul Basariya, S. Parvathy, and S. Prabhakar, "Removal of Cr (VI) by electrochemical reduction," *Sep. Purif. Technol.*, vol. 60, no. 1, pp. 96–102, 2008, d https://doi.org/10.1016/j.seppur.2007.07.053.

[30] A. Ahmadi, S. Heidarzadeh, A. R. Mokhtari, E. Darezereshki, and H. A. Harouni, *Optimization of heavy metal removal from aqueous solutions by maghemite (γ-Fe2O3) nanoparticles using response surface methodology*. Elsevier B.V., 2014, https://doi.org/10.1016/j.gexplo.2014.10.005.

[31] Kunwar P., A. K. Singh, U. V. Singh, and P. Verma, "Optimizing removal of ibuprofen from water by magnetic nanocomposite using Box-Behnken design," *Environ. Sci. Pollut. Res.*, vol. 19, no. 3, pp. 724–738, 2012, https://doi.org/10.1007/s11356-011-0611-4.

[32] S. Polat and P. Sayan, "Application of response surface methodology with a Box–Behnken design for struvite precipitation," *Adv. Powder Technol.*, vol. 30, no. 10, pp. 2396–2407, 2019, https://doi.org/10.1016/j.apt.2019.07.022.

[33] J. Yan, T. Wei, J. Cheng, Z. Fan, and M. Zhang, "Preparation and electrochemical properties of lamellar MnO2 for supercapacitors," *Mater. Res. Bull.*, vol. 45, no. 2, pp. 210–215, 2010, https://doi.org/10.1016/j.materresbull.2009.09.016.

[34] M. Ghaemi, L. Khosravi-Fard, and J. Neshati, "Improved performance of rechargeable alkaline batteries via surfactant-mediated electrosynthesis of MnO2," *J. Power Sources*, vol. 141, no. 2, pp. 340–350, 2005, https://doi.org/10.1016/j.jpowsour.2004.10.004.

[35] A. Xie *et al.*, "A coralliform-structured γ-MnO2/polyaniline nanocomposite for high-performance supercapacitors," *J. Electroanal. Chem.*, vol. 789, pp. 29–37, 2017, https://doi.org/10.1016/j.jelechem.2017.02.032.

[36] R. Liu and S. B. Lee, "MnO2/poly (3, 4-ethylenedioxythiophene) coaxial nanowires by one-step coelectrodeposition for electrochemical energy storage," *J. Am. Chem. Soc.*, vol. 130, no. 10, pp. 2942–2943, 2008, https://doi.org/10.1021/ja7112382.

[37] Z. M. Issa and R. H. Salman, "Chromium Ions Removal by Capacitive Deionization Process : Optimization of the Operating Parameters with Response Surface Methodology," *J. Egological Eng.*, vol. 24, no. 1, pp. 51–65, 2023, https://doi.org/10.12911/22998993/155953.

[38] W. Menke, "Review of the Generalized Least Squares Method," *Surv. Geophys.*, vol. 36, no. 1, pp. 1–25, 2015, https://doi.org/10.1007/s10712-014-9303-1.

[39] H. Singh, S. Sonal, and B. K. Mishra, "Hexavalent chromium removal by monopolar electrodes based electrocoagulation system: optimization through Box–Behnken design," *J. Water Supply Res. Technol.*, vol. 67, no. 2, pp. 147–161, 2018, https://doi.org/10.2166/aqua.2017.135.

[40] U. K. Garg, M. P. Kaur, D. Sud, and V. K. Garg, "Removal of hexavalent chromium from aqueous solution by adsorption on treated sugarcane bagasse using response surface methodological approach," *Desalination*, vol. 249, no. 2, pp. 475–479, 2009, https://doi.org/10.1016/j.desal.2008.10.025.

[41] B. Ayoubi-Feiz, S. Aber, A. Khataee, and E. Alipour, "Electrosorption and photocatalytic one-stage combined process using a new type of nanosized TiO2/activated charcoal plate electrode," *Environ. Sci. Pollut. Res.*, vol. 21, pp. 8555–8564, 2014, https://doi.org/10.1007/s11356-014-2777-z.

[42] P. Mohanraj, J. S. S. Allwin Ebinesar, J. Amala, and S. Bhuvaneshwari, "Biocomposite based electrode for effective removal of Cr (VI) heavy metal via capacitive deionization," *Chem. Eng. Commun.*, vol. 207, no. 6, pp. 775–789, 2020, https://doi.org/10.1080/00986445.2019.1627338.

[43] P. Rana-Madaria, M. Nagarajan, C. Rajagopal, and B. S. Garg, "Removal of chromium from aqueous solutions by treatment with carbon aerogel electrodes using response surface methodology," *Ind. Eng. Chem. Res.*, vol. 44, no. 17, pp. 6549–6559, 2005, https://doi.org/10.1021/ie050321p.

[44] L. Huang *et al.*, "Study on mechanism and influential factors of the adsorption properties and regeneration of activated carbon fiber felt (ACFF) for Cr(VI) under electrochemical environment," *J. Taiwan Inst. Chem. Eng.*, vol. 45, no. 6, pp. 2986–2994, 2014, https://doi.org/10.1016/j.jtice.2014.08.013.

[45] Y. Chen *et al.*, "Removal of trace Cd(II) from water with the manganese oxides/ACF composite electrode," *Clean Technol. Environ. Policy*, vol. 17, no. 1, pp. 49–57, 2015, https://doi.org/10.1007/s10098-014-0756-1.

[46] Y. X. Liu, D. X. Yuan, J. M. Yan, Q. L. Li, and T. Ouyang, "Electrochemical removal of chromium from aqueous solutions using electrodes of stainless steel nets coated with single wall carbon nanotubes," *J. Hazard. Mater.*, vol. 186, no. 1, pp. 473–480, 2011, https://doi.org/10.1016/j.jhazmat.2010.11.025.

[47] P. P. Mashile, M. K. Dimpe, and P. N. Nomngongo, "Application of waste tyre-based powdered activated carbon for the adsorptive removal of cylindrospermopsin toxins from environmental matrices : Optimization using response surface methodology and," *J. Environ. Sci. Heal. Part A*, pp. 1–7, 2019, https://doi.org/10.1080/10934529.2019.1579538.

[48] A. Islam, Z. Nikoloutsou, and V. Sakkas, "Statistical optimisation by combination of response surface methodology and desirability function for removal of azo dye from aqueous solution," *Int. J. Environ. Anal. Chem.*, vol. 90, no. 3–6, pp. 497–509, 2010, https://doi.org/10.1080/03067310903094503.

[49] N. M. K. Chockalingam and R. P. K. Kalaiselvan, "Optimization of CNC-WEDM Parameters for AA2024 / ZrB2 in situ Stir Cast Composites Using Response Surface Methodology," *Arab. J. Sci. Eng.*, 2020, https://doi.org/10.1007/s13369-020-04490-x.

الامتزاز الكهربائي لأيونات الكروم السداسية التكافؤ بواسطة القطب المركب من MnO$_2$ /ألياف الكربون: تحليل العملية وتحسينها من خلال تصميم Box-Behnken

زينب محمد عيسى [١، *] **، رشا حبيب سلمان** [١] **، وبراشانت باسافاراج** [٢]

١ قسم الهندسة الكيمياوية، كلية الهندسة، جامعة بغداد، العراق
٢ جامعة بالكوت، الهند

الخلاصة

تناولت هذة الدراسة طريقة تحضير قطب نانوي مركب (ألياف الكربون/ MnO$_2$) ، حيث تم ترسيب ثاني أكسيد المنغنيز ذو البنية النانوية على سطح ألياف الكربون (CF) باستخدام طريقة بسيطة تدعى الترسيب الكهربائي الأنودي. تم تشخيص الأقطاب المركبة الناتجة بأستخدام الفحص المجهري الإلكتروني (FESEM) لدراسة شكل المادة النانوية المتكونة على سطح القطب وفحص حيود الأشعة السينية (XRD) لدراسة التركيب البلوري للمادة المتكونة على السطح. هنالك عدد قليل جدًا من الدراسات التي قامت بدراسة كفاءة القطب المحضر MnO$_2$ / CF في إزالة المعادن الثقيلة، وخاصة الكروم. تم فحص خصائص الامتزاز الكهربائي للقطب النانوي MnO$_2$ / CF عن طريق إزالة أيونات (Cr (VI من محلول مائي. لدراسة تأثير العوامل التشغيلية المختلفة والتفاعل فيما بينها على كفاءة عملية الازالة، تم اختيار درجة الحموضة وتركيز كلوريد الصوديوم وجهد الخلية كظروف تشغيلية. باستخدام تصميم Box-Behnken (BDD)، أظهرت النتائج أنه عند الرقم الهيدروجيني = ٢ ، جهد الخلية = ٤,٦ فولط وتركيز كلوريد الصوديوم = ١,٥ جم / لتر تم تحقيق الظروف المثلى لإزالة أيونات (Cr (VI. في هذه الدراسة تم تحقيق كفاءة عالية في ازالة أيونات (Cr (VI بأستخدام قطب ألياف الكربون/ MnO$_2$ وأن طريقة BBD كانت استراتيجية مجدية وفعالة لتقييم البيانات التجريبية في ظروف مختلفة.

الكلمات الدالة: عملية الامتزاز الكهربائي، أيونات الكروم سداسية التكافؤ، القطب المركب، الترسيب الكهربائي، التركيب النانوي MnO$_2$، تصميم Box-Behnken.